Catalysis Science & Technology

Accepted Manuscript

This is an *Accepted Manuscript*, which has been through the Royal Society of Chemistry peer review process and has been accepted for publication.

Accepted Manuscripts are published online shortly after acceptance, before technical editing, formatting and proof reading. Using this free service, authors can make their results available to the community, in citable form, before we publish the edited article. We will replace this *Accepted Manuscript* with the edited and formatted *Advance Article* as soon as it is available.

You can find more information about *Accepted Manuscripts* in the Information for Authors.

Please note that technical editing may introduce minor changes to the text and/or graphics, which may alter content. The journal's standard Terms & Conditions and the Ethical guidelines still apply. In no event shall the Royal Society of Chemistry be held responsible for any errors or omissions in this *Accepted Manuscript* or any consequences arising from the use of any information it contains.

ROYAL SOCIETY OF CHEMISTRY

www.rsc.org/catalysis

Catalysis Science & Technology

ARTICLE

The influence of catalyst amount and Pd loading on the H_2O_2 synthesis from hydrogen and oxygen

Received 00th January 20xx,
Accepted 00th January 20xx

DOI: 10.1039/x0xx00000x

www.rsc.org/

Nicola Gemo[a,b], Stefano Sterchele[b,c], Pierdomenico Biasi[b,d],†, Paolo Centomo[c], Paolo Canu[a], Marco Zecca[c], Andrey Shchukarev[d], Krisztián Kordás[e], Tapio O. Salmi[b], Jyri-Pekka Mikkola[b,d]

Abstract: Palladium catalysts with an active metal content from 0.3 to 5.0 wt.% and supported on a strongly acidic, macroporous resin were prepared by ion-exchange/reduction method. H_2O_2 direct synthesis was carried out in the absence of promoters (acids and halides). The total Pd amount in the reacting environment was varied by changing A) the catalyst concentration in the slurry and B) the Pd content of the catalyst. In both cases, smaller amounts of the active metal enhance the selectivity towards H_2O_2, at any H_2 conversion, with option B) better than A). In case A), the Pd(II)/Pd(0) molar ratio (XPS) in the spent catalysts was found to decrease at lower catalyst Pd content. With these catalysts and this experimental set-up the dynamic H_2^L/Pd molar ratio, the metal loading and the metal particle size were the key factors controlling the selectivity, which reached 57 % at 60 % H_2 conversion, and 80 % at lower conversion

Keywords: Hydrogen peroxide direct synthesis, Pd catalyst, Oxidation state, nanoparticle size, Hydrogen/Palladium ratio, resin catalysts

.

Introduction

Hydrogen peroxide is considered one of the most environmentally friendly and efficient oxidizing agents available to the industry. Its direct production from H_2 and O_2 (direct synthesis, DS) has been attracting considerable interest because of the potentially reduced costs and flexibility of its process[1, 2] . Although the DS is the simplest route to H_2O_2, the reaction involves multiple paths, Scheme 1, with consecutive and parallel reactions leading to water, which is by far thermodynamically favored. This adversely affects the selectivity and limits the yield of H_2O_2.

Therefore, the selectivity towards H_2O_2 is the first issue for a viable industrial application. Many Authors investigated the reaction conditions, trying to suppress the undesired side reactions[3-13] . The hydrogenation of hydrogen peroxide appears the major route of its consumption [14-18] . Catalyst design is the main tool to improve the selective synthesis of H_2O_2 [10, 19] . Researchers investigated the catalyst properties to limit the undesired side reactions [1, 13] . Pd has proven to be the best active metal, also on standard supports such as carbon, SiO_2 or Al_2O_3. Mineral acids and halides (either Cl^- or Br^-) are known to be effective selectivity enhancers [1, 13] , especially when combined to each other, but corrosion and metal leaching could ensue from their use. In addition, halide ions can be detrimental in down-stream applications. The oxidation state of palladium has been recognized to affect the selectivity. However, there is not yet consensus on its actual active form during the H_2O_2 DS. According to Choudhary *et al.* [20, 21] PdO is the active form, whereas Fierro *et al.* [22] concluded that Pd(II) ions are most selective towards H_2O_2 when a Pd catalyst supported on a strongly acidic resin was used. Burato *et al.*[23] adopted the same catalyst formulation as Fierro's one, but trasformed it into Pd(0) upon pre-reduction of the metal; they suggest that the metallic nanoparticles are the most active for peroxide formation. More recently, Edwards *et al.*[19] reported that the Pd(0) is mainly responsible for the hydrogenation reaction, whereas Pd(II) is active in producing the peroxide. Melada *et al.*[24] investigated Pd supported on a

[a] Dr. N. Gemo, Prof. P. Canu
Dipartimento di Ingegneria Industriale, University of Padova
via Marzolo 9, 35131, PADOVA, Italy
[b] Dr. N. Gemo, Dr. P. Biasi, Prof. T. Salmi, Prof. J.-P. Mikkola Department of Chemical Engineering
Åbo Akademi University
Biskopsgatan 8, ÅBO-TURKU, 20500, Finland
[c] Dr. S. Sterchele, Dr. P. Centomo, Prof. M. Zecca
Dipartimento di Scienze Chimiche
University of Padova
via Marzolo 8, 35131, PADOVA, Italy
[d] Dr. P. Biasi, Dr. A. Shchukarev, Prof. J.-P. Mikkola
Department of Chemistry
Umeå University
SE-90187 UMEÅ, Sweden
[e] Dr. K. Kordás
Microelectronics and Materials Physics Laboratories
University of Oulu
FI-90014 OULU, Finland
† E-mail: bpierdom@abo.fi

Electronic Supplementary Information (ESI) available: [details of any supplementary information available should be included here]. See DOI: 10.1039/x0xx00000x

Catalysis Science & Technology Accepted Manuscript

Please do not adjust margins

modified zirconia, exposing the reduced catalyst to mildly oxidizing conditions, and they concluded that reduced Pd nanoparticles with a PdO-rich surface favored the H_2O_2 direct synthesis. More recently, Lunsford *et al.*[25] observed no activity over the oxidized form of a Pd/SiO_2 catalyst, but 60% selectivity was obtained with the reduced form of this catalyst. In this context, subtle changes in the active nanoparticles surface during the reaction should be tackled. For instance, the oxidation state could be affected by the reaction environment and the metal nanoparticle size, in particular if it changes during the reaction. This problem is still a matter of debates in the H_2O_2 community. Only very recently the influence of reaction conditions on the catalyst state has attracted some attention. In a very recent study, Arrigo *et al*[26] reported that variations of the catalyst features at reaction conditions affect the performance and features of the catalyst.

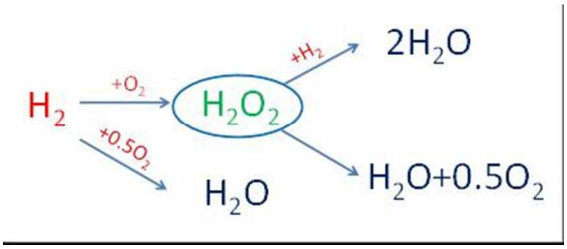

Scheme 1. Reactions involved in the direct synthesis of H_2O_2.

In this study, we report on the performance of palladium catalysts supported on a strongly acidic resin[22] (Lewatit K2621) and used with addition of no promoter.

Catalyst characterizations were performed on the fresh and spent catalysts. A strongly acidic resin (Lewatit K2621)[24, 25, 29, 30] was used to synthesize catalysts with different Pd loadings, ranging from 0.3 to 5.0 wt.%. These catalysts already demonstrated good selectivity in the H_2O_2 DS[22-24] . The correlation between the metal nanoparticles size, the H_2/Pd ratio, the oxidation state of the catalyst and its activity towards the hydrogen peroxide direct synthesis is discussed. The size distribution and oxidation state of Pd nanoparticles were provided by TEM and XPS.

The ultimate focus of this work is on the reaction mechanism, still uncertain, where the role of the Pd/H_2 ratio on the selectivity appears a key factor. Here, the aim of the work is to understand if the reactions involved are structure sensitive, trying to get more insights in the understanding of this challenging reaction mechanism.

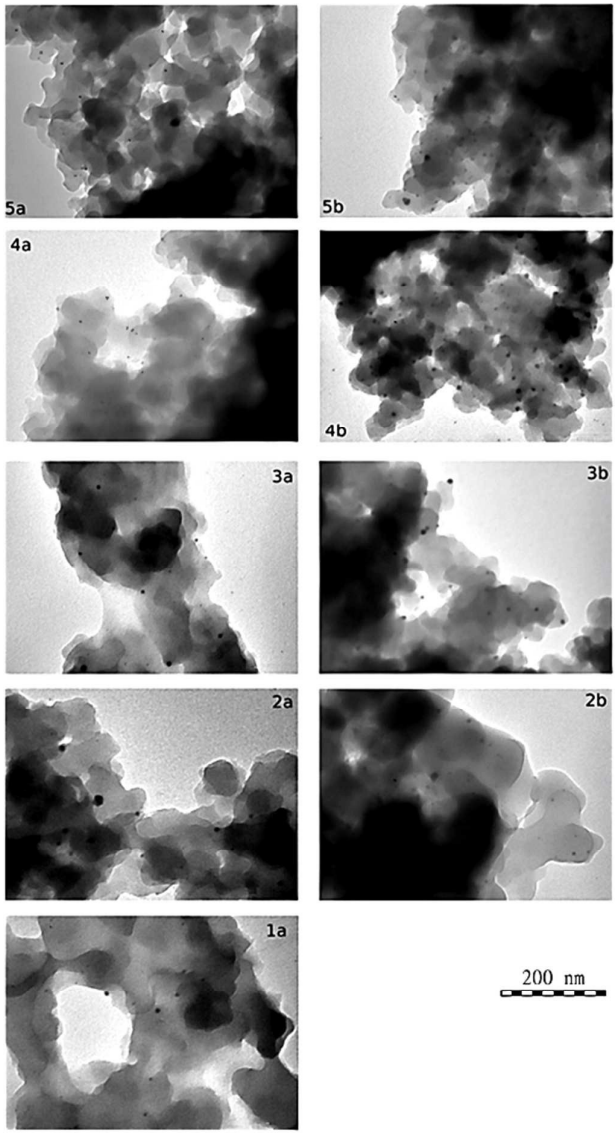

Figure 1. TEM images of the X-Pd/K2621 catalysts (a: fresh, left side; b: spent, right side) with different Pd loadings: 1) 0.3-Pd/K2621; 2) 0.5-Pd/K262; 3) 1.0-Pd/K2621; 4) 2.5-Pd/K2621; 5) 5.0-Pd/K2621.

Results and Discussion

Catalyst Characterization method

TEM images, Figure 1, illustrate the morphological properties of the Pd nanoparticles in the X-Pd/K2621 catalysts (X=0.3, 0.5, 1.0, 2.5 and 5.0 represents the Pd wt.%), before and after use. Spherical nanoparticles uniformly distributed in the support are observed for all the catalysts. The particle size distributions determined from image analysis are shown in Figure 2.

Catalysis Science & Technology Accepted Manuscript

This journal is © The Royal Society of Chemistry 20xx

Please do not adjust margins

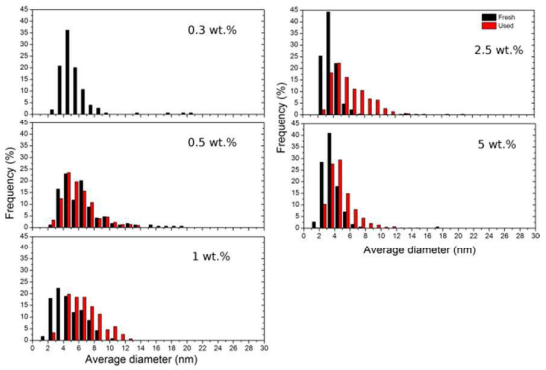

Figure 2. Particle size distribution of the Pd/K2621 catalysts with different Pd loading, before (dark) and after (red) the reaction.

Table 1. Pd oxide content and average nanoparticle size of fresh and spent catalysts

Cat.	Nanoparticle size			Pd dispersion (%) [a]		Pd(II)/Pd(0)	
Pd (%)	Fresh (nm)	Spent (nm)	Difference (%)	Fresh	Spent	Fresh	Spent
0.3	4.7	/	/	27.3	/	/	/
0.5	5.3	5.5	+4	24.5	23.7	/	0.80
1.0	4.5	6.4	+42	28.4	20.6	2.67	1.43
2.5	3.6	5.2	+44	34.6	25.0	2.75	3.30
5.0	3.1	4.3	+39	39.3	29.6	4.36	5.80

a: estimated (see Supporting Material, Section 1)
/: data unavailable

Nanoparticles diameter ranged from 2 to 12 nm. The average nanoparticles diameters are summarized in Table 1. Interestingly, the nanoparticles size of the fresh catalyst shifts to smaller values as the amount of palladium increased. This could be explained by the features of the acid groups of the resin. In the catalysts with the higher Pd content, ion-exchange of the Pd(II) ions involved the sulfonic groups located both on the pores walls and in the layer just beneath them, which is to some extent swollen and accessible in the aqueous environment[27, 28] . Hence, in the subsequent reduction step, a sensible fraction of the metal nanoparticles was formed within the polymer framework, efficiently limiting their growth. On the contrary, at low metal content, the Pd(II) ions are exchanged only by the sulfonic groups on the pore walls. As a consequence, the polymer framework was less efficient in controlling the nanoparticle size. All the spent catalysts show a particle size distribution broader and shifted towards larger values, Figure 2 and Table 1, suggesting some aggregation during the reaction. A similar investigation was reported by Ouyang et al. [29] , with slightly different results due to the different supports used. Probably the different particle sizes obtained in the present work (with different Pd loadings) are to be ascribed to the pores distribution inside the resin, its ability to be swollen in liquid phase and the sulfonic groups. As expected, the catalysts with the highest Pd content were most affected, showing approx. 40% of nanoparticles size increase, whereas sintering was negligible in the 0.5 wt.% catalyst (the lowest Pd content).

The dispersion of the metal phase was estimated as the percent ratio between surface and total Pd atoms from the average nanoparticle size, assuming that a) the metal nanoparticles were spherical, b) Pd had the fcc structure typical of the bulk and c) Pd atomic radius is 137 pm (see Supporting Material, Section 1, for further details). The estimated dispersion values (Table 1) were in the range 25-40 %, with a less than two-fold change from the least to the most dispersed catalyst (Supporting Material, Figure 1).

The XPS spectra for the fresh and spent 5.0-Pd/K2621 catalyst are reported in Figure 3 (other catalysts' spectra are similar).

XPS can sample Pd down to approx. 10 nm below the metal surface, as can be calculated by established correlation[30] . Since the metal nanoparticles in our catalysts had diameters in the range of 3-6.5 nm (Table 1), we can assume that their XPS analysis is representative of most of their volume. The spectra before and after the reaction (Figure 4) compare well, although a decrease in the intensity of the Pd 3d core level was observed, possibly due to the effect of Pd nanoparticle size on the binding energy (BE), as commented below. Signals from carbon, oxygen, sulfur and nitrogen were found in addition to the palladium one. Sulfur is present in the sulfonic groups of the polymeric support catalysts and nitrogen could stem from the nitrate ions of the metal precursor used in the ion-exchange step. In fact the position of the nitrogen peak (ca 400 eV) suggests the presence in the samples of ammonium ions, possibly obtained by reduction of NO_3^- during the reduction step[31].

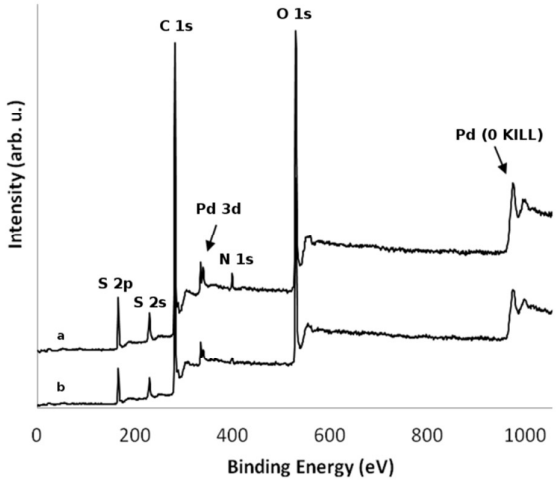

Figure 3. XPS spectra of the 5.0 Pd/K2621 catalyst: a) fresh; b) used

Figure 4 shows the high-resolution XPS spectra of the Pd 3d core level. The binding energy of Pd $3d_{5/2}$ photoelectron line in metallic Pd and in Pd(II) fall at 335.1 and 336.3 eV, respectively [32] . In the fresh catalyst two peaks for the Pd $3d_{5/2}$ signals were

Catalysis Science & Technology Accepted Manuscript

Please do not adjust margins

observed at 336.0 eV and 337.8 eV, indicating that Pd is present in two different oxidation states; both binding energies are higher than reported in the literature. However, the positive shift of 1 eV in the BE has already been reported by Penner *et al*.[33] for small Pd(0) and Pd(II) nanoparticles (2-10 nm). Both the BE shift and the nanoparticle size observed for our catalysts compare well with the values reported by Penner *et al*.[33] , hence the two peaks can be attributed to Pd(0) and Pd(II), respectively. A third peak observed around 344.8 eV corresponds to energy loss features. For each sample, the signals of the Pd(3d) core level were deconvoluted into two curves, the integration of which allowed the estimation of the Pd(II)/Pd(0) atomic ratio in the catalysts. Estimated values are

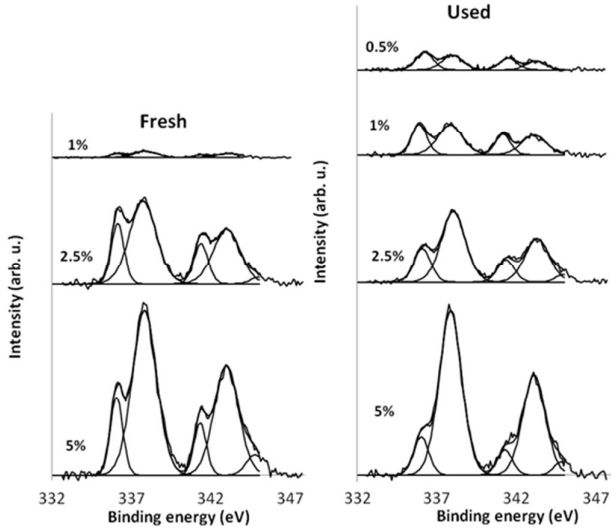

reported in Table 1. In the fresh catalysts with Pd content ≥1.0 wt.% this ratio was higher than 1, showing that Pd was mostly present in the oxidized form.

Figure 4. XPS signals of Pd 3d core level in the X Pd/K2621 fresh (left) and spent (right) catalysts (X is the Pd wt.%, reported in each panel).

The data of Table 1 show that in the fresh catalyst the higher the Pd amount , the higher the dispersion and the oxidation degree. The oxidation degree still increases with the Pd amount also in the spent catalyst, but the Pd(II)/Pd(0) ratio changes during the reaction and at least in one case (1.0-Pd/K2621) a partial reduction of the metal is observed. With the highest Pd amounts in the catalysts (2.5-Pd/K2621 and 5.0-Pd/K2621) further oxidation of the metal is evident at the end of the reaction.

Table 2. Summary of the experimental conditions and the main results at X_{H2}=0.6

	Catalyst			[Pd]	H_2^t / Pd	Selectivity	H_2O_2 productivity	H_2O productivity
#	ID	mass (g)	Pd (μmol)	(μM)	(mol/mol)	(%)	$\cdot 10^3$ (mol/h)	$\cdot 10^3$ (mol/h)
1	1.0-Pd/K2621	0.075	7	16.7	530	24	2.33	7.20
2	1.0-Pd/K2621	0.11	10	23.8	423	24	4.71	14.81
3	1.0-Pd/K2621	0.15	14	33.3	299	23	12.76	41.82
4	1.0-Pd/K2621	0.3	28	66.7	173	16	10.22	54.80
5	1.0-Pd/K2621	0.5	47	111.9	92	12	16.71	123.84
6	0.3-Pd/K2621	0.15	4	9.5	1011	45	5.89	7.19
7	0.5-Pd/K2621	0.15	7	16.7	530	57	12.39	9.30
8	2.5-Pd/K2621	0.15	35	83.3	99	22	16.22	58.83
9	5.0-Pd/K2621	0.15	71	169.0	47	10	16.63	148.01

Activity in the H_2O_2 direct synthesis

A summary of the main results of the catalytic tests is reported in Table 2. The experiments with different concentration of the same catalyst in the slurry (1 to 5) will be presented first, and separately from those where the same amount of different catalysts was used (3, 6 to 9). A common discussion will follow.

Changing the catalyst concentration in the slurry

The evolution of H_2O_2 and H_2O concentrations and of H_2O_2 selectivity varying the amounts of the 1.0-Pd/K2621 (Table 2, runs 1 to 5) are reported in Figure 5. H_2O was always the main product, with H_2O_2 selectivity values never exceeding 30%. As expected, the larger the [Pd] in the reactor, the higher the reaction rates. But the highest selectivity and final H_2O_2 concentration (7-8 mM) values were achieved with the smallest concentration of catalyst (hence of Pd) in the reaction mixture. In these cases, the selectivity initially increases, reaching a maximum after ca. 10 minutes and then decreases steadily. With higher [Pd], the initial increase of selectivity is too fast, appearing to decrease from the very beginning of the

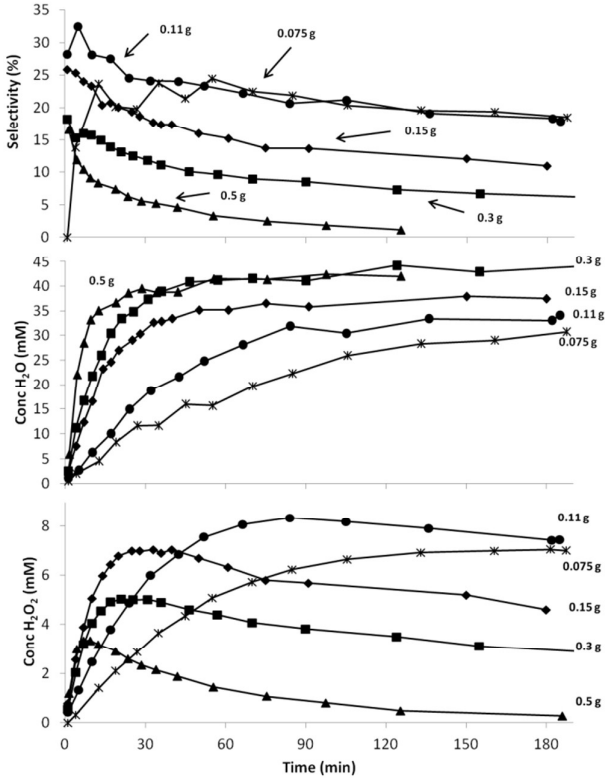

reaction. The drop in selectivity is larger with higher catalyst concentration. Further comments follow in the common discussion.

Figure 5. H_2O_2 selectivity and H_2O_2 and H_2O concentration with different concentration of 1.0 Pd/K2621 catalyst in the slurry: * 0.075 g; ● 0.110 g; ♦ 0.150 g; ■ 0.300 g; ▲ 0.500 g.

Changing the Pd loading in the catalyst

The evolution of H_2O_2 and H_2O concentrations and of H_2O_2 selectivity varying the Pd loading within the same amount of

Catalysis Science & Technology Accepted Manuscript

This journal is © The Royal Society of Chemistry 20xx

Please do not adjust margins

catalyst in the slurry (Table 2, runs 3 and 6 to 9) are reported in Figure 6. Again, in these experiments the highest and lowest selectivity values were obtained with the lowest and the highest Pd concentration in the reaction environment, respectively. Note that using the strategy of different Pd loadings both the H_2O_2 concentration and the selectivity were higher than simply decreasing the catalyst amount (Figures 5 and 6).

The selectivity of the 0.3-Pd/K2621 and 0.5-Pd/K2621 catalysts topped 80 % after ca. 10 min and dropped to a final value of approx. 40 %, which is higher than the final value in any of the experiments of the first set. These two catalysts yield a final concentration of H_2O_2 up to 14.6 mM (without any promotion by acids and/or halides). Generally speaking, this is a quite low concentration, but it is due to the low overall H_2 amount introduced in the reactor. Moreover, the use of the same palladium concentration with different catalysts leads to much better results when the metal load in the support is lower (Table 2, runs 1 and 7).

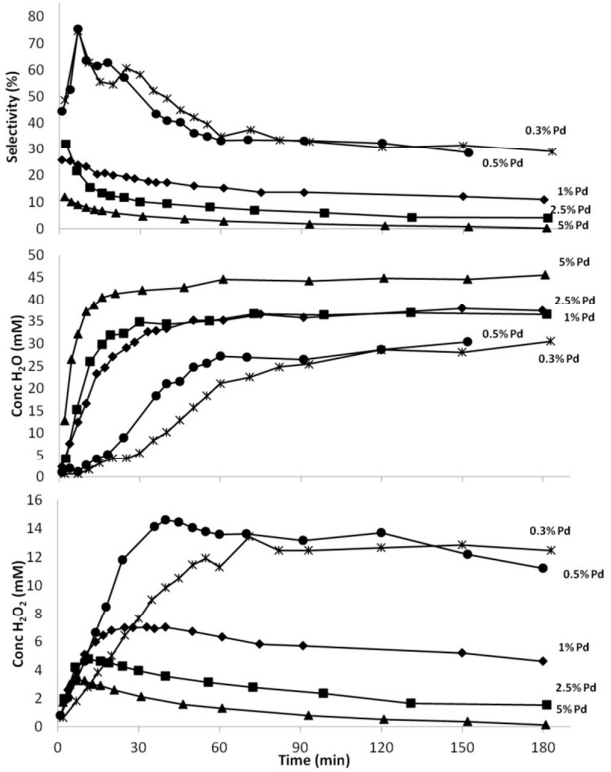

Figure 6. H_2O_2 selectivity and H_2O_2 and H_2O concentration with the same amount of different catalysts: * 0.3 Pd/K2621; ● 0.5 Pd/K2621; ♦ 1.0 Pd/K2621; ■ 2.5 Pd/K2621; ▲ 5.0 Pd/K2621.

Comparison with other catalysts

A comparison with literature productivity data is not trivial, because reaction conditions might differ and H_2 conversion (X_{H2}) results not always are reported. Unfortunately, different research groups normally operate at different experimental conditions[1, 13, 34], so that an ideal comparison is almost impossible. However, a comparison based on the specific H_2O_2 productivity, i.e. the ratio between the peroxide production rate and the Pd amount, can give interesting information. Note that the specific productivity is often referred as turnover frequency, TOF, although the ratio is only an approximation of the microscopic TOF, and its definition questionable in a multisteps reaction. Literature data are reported in Table 3.

In our conditions the specific H_2O_2 productivity spans from 234 (5.0-Pd/K2621) to 1770 (0.5-Pd/K2621) $mol_{H2O2}/(mol^{Pd}\cdot h)$ at $X_{H2}=0.6$. These results compare well with the highest ones reported in the literature, if conveniently scaled with the total pressure, that boosts the reaction rates. Note that we achieved such performances without promoters (mineral acids and/or halide ions) in the reaction environment and at fairly low pressure. The selectivity and the productivity are comparable to those achieved using selectivity enhancers, indicating the effectiveness of the catalyst synthesized.

Catalysis Science & Technology Accepted Manuscript

Please do not adjust margins

Table 3. Comparison between this work and literature results.

Ref	Catalyst	Reactor	Liquid Phase	Gas Composition [%]	T [°C]	P [bar]	Additives	Productivity [mol H_2O_2 / (molPd·h)]	Selectivity [%]	H_2 conv. [%]
This work	0.3÷5.0%Pd/K2621	Batch	CH_3OH	$H_2:O_2:CO_2$ = 4:20:76	2	19.5	/	1770÷234	57÷10	60
35	2.5%Pd-2.5%Au/Carbon	Batch	$CH_3OH:H_2O$ = 1.93	$H_2:O_2:CO_2$ = 3.6:7.1:89.3	2	37	/	304	80	/
	2.5%Pd-2.5%Au/Silica							298	80	/
36	1.8%Pd-2.5%Au/HZSM-5	Batch	$CH_3OH:H_2O$ = 1.93	$H_2:O_2:CO_2$ = 3.6:7.1:89.3	2	37	/	467	/	/
37	1.22%Pd-0.92%Au/S-ZrO_2	Semibatch	CH_3OH	$H_2:O_2$ = 4:96	20	1	H_2SO_4 (0.03 M)	90	62	64
	1.3%Pd-0.2%Pt/S-ZrO_3							124	65	64
24	2.64%Pd/ZS	Semibatch	CH_3OH	$H_2:O_2$ = 4:96	20	1	H_2SO_4 (0.03 M)	58.5	40	99.5
38	1.6%Pd/SiO_2 (HSO_3-functionalized)	Semibatch	CH_3OH	$H_2:O_2:N_2$ = 3.6:46.4:50	40	95	HBr	1857	83	> 90
3	5%Pd/C	Semibatch	H_2O	$H_2:O_2:CO_2$ = 4:16:80	60	80	H_3PO_4 (0.004 M) NaBr (0.03 M)	5632	74	29
39	4.4%Pd/SBA15	Semibatch	CH_3OH	$H_2:O_2:CO_2:N_2$ = 7.7:15.4:61.5:15.4	20	6.5	H_2SO_4 (0.03 M)	282	40	/
12	0.5%Pd-0.5%Au/TiO_2	Continuous	$CH_3OH:H_2O$ = 1.94	$H_2:O_2:CO_2$ = 4:4:92	2	10	/	26	23	18
40	2.12%Pd/ZrO_2	Continuous	CH_3OH	$H_2:O_2:CO_2$ = 2:18:80	-10	10	/	4	45	15

This journal is © The Royal Society of Chemistry 20xx

Please do not adjust margins

Catalysis Science & Technology Accepted Manuscript

Mass transfer limitations

The experiments were performed varying the amount of the active metal, in two different ways. The reaction rates varied accordingly, as clearly shown in Figure 5 and Figure 6, being quite fast in some cases, so that concerns of mass transfer limitations may arise. Hence, H_2 consumption rate was related to the active metal amount: would the mass transfer be limiting, increasing the amount of catalyst should not bring any improvement in the conversion rate. However, a linear relation was observed between H_2 consumption rate and catalyst amount (Supporting material, Section 2), clearly proving that the reactions are occurring under the kinetic regime, as already demonstrated in comparable conditions[14]. The H_2 mass transfer limitation was also experimentally excluded in our previous work [41], where the presence of H_2 in the bulk of the liquid phase was experimentally observed in conditions comparable to those of this work. Would the reactor be limited by mass transfer phenomena, the presence of H_2 in the bulk of the liquid phase should not have been observed. Moreover, in a stirred slurry reactor, values of mass transfer coefficient about 10 min^{-1} have been measured[6]. Hence, the H_2 transfer rate would be approximately 70 mmol/min at our experimental conditions. The maximum H_2 consumption rate that we measured was 3 mmol/min (supplementary figure 3), once again concluding that H_2 mass transfer limitation can be excluded.

Disproportionation kinetics

The analysis of the H_2 consumption rate helps to clarify the role of each reaction of Scheme 1 during the experiments. The highest H_2O_2 concentration obtained (Figure 5 and Figure 6) always corresponds to the complete H_2 consumption. Hence, according to the stoichiometry of the reactions, the subsequent slow H_2O_2 depletion (if any) is due only to the disproportionation reaction. This is clearly much slower than all the other reactions, as already demonstrated[14]. A quantitative estimation of the first-order disproportionation kinetic constants is given in the Supporting Material, Section 3.

Activity and selectivity

In a batch reactor the production rate and the selectivity vary over time. This is a consequence of variations in the reaction environment during the reaction, i.e. the reagents and product concentrations (Scheme 1). In this work, the production rates and the selectivity values were compared at a fixed H_2 conversion (60%, see Supporting material, Section 2 for motivations) rather than at a fixed reaction time. Though the latter convention is frequently used, Figure 5 and Figure 6 clearly show how misleading it could be, if one compares selectivities at a fixed time, e.g. 1h. Hence, catalysts have been compared at the same H_2 conversion, high enough to ensure appreciable rates of the consecutive undesired reactions, if any. The production rates of H_2O_2 ($R_{60}^{H_2O_2}$)and H_2O ($R_{60}^{H_2O}$) at 60% H_2 conversion were calculated as the slopes of the time profiles of H_2O_2 and H_2O concentrations (Figure 5 and Figure 6) up to $x_{H2}=0.6$ (achieved at very different reaction times). Selectivity values were compared as well. These are cumulative values, from the beginning up to 60% H_2 conversion, hence they can differ from the actual instant values at that conversion. However, since the H_2O_2 and especially H_2O concentration profiles were quite linear up to $x_{H2}=0.6$, cumulative and instant productivities and selectivities should match reasonably.

Values are reported in Table 2 and in Figure 7 as a function of the concentration of Pd in the reaction mixture. $R_{60}^{H_2O}$ increases linearly with the amount of palladium in both sets of experiments, whereas $R_{60}^{H_2O_2}$ does it only raising the total amount of the same catalyst (Figure 7). When the same catalyst is used in different amounts, the metal nanoparticles are the same, having always the same initial size and initial Pd(II)/P(0) ratio. This implies that the metal surface has always the same features and the only changing parameter is the total surface area available, directly proportional to the total concentration of palladium in the reaction environment. We can conclude that in runs 1 to 5 (Table 2) both $R_{60}^{H_2O_2}$ and $R_{60}^{H_2O}$ were directly proportional to the metal surface area, as expected for a reaction occurring under the kinetic regime. Although the rates of formation of both products vary linearly with the palladium concentration, $R_{60}^{H_2O}$ increases more rapidly, depressing the selectivity. Therefore it is clear that the more palladium is used the more water is relatively produced.

When the total concentration of palladium is changed by using equal amounts of catalysts with different metal loads, only $R_{60}^{H_2O}$ linearly depends on the palladium concentration, but $R_{60}^{H_2O_2}$ does not. In particular when the metal load in the catalyst is 0.5 % or more, only a very slight increase of $R_{60}^{H_2O_2}$ is observed and the ratio between its highest and lowest values is less than 3. By contrast, there is a 20-fold increase in $R_{60}^{H_2O}$ from the catalyst with the lowest water productivity to the most productive one. As the consequence, the decrease of the selectivity towards H_2O_2 from the most to the least selective catalyst is 5-fold as opposed to the 2-fold decrease observed changing the quantity of the same catalyst (first set of experiments). When using different metal loads, the total metal surface varies both with the catalyst palladium content and the size of the nanoparticles. However, the surface amount of palladium is directly proportional to the total amount of the metal even taking into account its different dispersion in the different catalysts (Supporting material, figure S2). Hence the palladium concentration can be taken as the only key parameter and it can be again concluded that the more palladium is used the lower is the selectivity.

The data above pinpoint that hydrogen peroxide production is structure sensitive while water production is not. Although final conclusions about the structure sensitivity require more detailed characterizations along the reaction course, being the measured rates apparent values arising from different reactions, this findings confirms previous studies related to the structure sensitivity[42-51] . In any case, it is clear that when different catalysts are used the nanoparticle size, the dispersion of the metal phase and the initial Pd(II)/Pd(0) ratio

Catalysis Science & Technology Accepted Manuscript

Please do not adjust margins

change from one experiment to another and must be taken into account. In particular, we observed that the higher the Pd load in the catalyst, the smaller the metal nanoparticle size (i.e. the higher the dispersion). Moreover, it seems that the catalysts with the smallest palladium nanoparticles are more rapidly oxidized (column 7, Table 2). This is even more clearly observed in the spent catalysts, where the Pd(II)/Pd(0) ratio increases upon decreasing the nanoparticle size. However, in the spent 1.0-Pd/K2621 the Pd(II)/Pd(0) ratio is lower than in the fresh catalyst. 2.5-Pd/K2621 and 5.0-Pd/K2621 behave the opposite. This further supports the conclusion that small metal nanoparticles can be more easily oxidized: during the reaction relatively large nanoparticles undergo a net oxidation, but the relatively small ones rather undergo a net reduction in spite of the abundance of oxygen in the reaction environment, especially in the late stage of the reaction. The relative role of Pd(II) and Pd(0) in the DS is a most debated one. Our results suggest that a catalyst highly oxidized is detrimental for the selectivity towards H_2O_2. It is therefore useful to operate under conditions where palladium reduction is favoured, as discussed later.

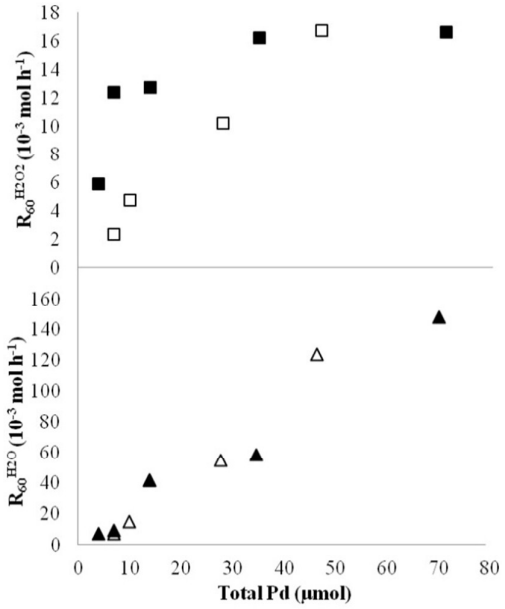

Figure 7. Production rates of H_2O_2, $R_{60}^{H_2O_2}$ (squares, above), and of water, $R_{60}^{H_2O}$ (triangles, below), with a) different amounts of 1.0-Pd/K2621 (open symbols) and b) with different X-Pd/K2621 catalyst (X= 0.3, 0.5, 1.0. 2.5, 5.0) (solid symbols).

As a final remark, one of the most probable explanation of the simultaneous increase of the Pd nanoparticles size and the decrease in the Pd(II)/Pd(0) molar ratio can be ascribed to the dissolution and re-deposition of Pd from small nanoclusters to bigger ones. However, the sintering effect can not be excluded, since it is a common behavior of nanoparticles in heterogeneous catalysis[26]. Both of the effects reported above (the Pd dissolution and re-deposition and the sintering effect) can result in an increase of the nanocluster size. TEM images before and after reaction suggested that these nanocluster changes can be explained by both the mechanisms reported above. The decrease in Pd(II)/Pd(0) molar ratio can also be explained by the Pd dissolution and re-deposition on the nanocluster[52]. The dissolution of Pd can be enhanced by H_2O_2, as already proved[53]. All These facts strongly support the idea that Pd is dissolved in the reaction medium during the H_2O_2 reaction and then re-deposited on the catalyst, raising the formation of bigger cluster size[54]. Moreover, sintering effect is detrimental for H_2O_2 direct synthesis[26], and in the present work we are showing that the catalyst that is not increasing its nanocluster size is the one that is best performing (table 1 and Figure 6).

H_2^L/Pd ratio

The importance of controlling the oxidation state of palladium in the catalyst prompted us to investigate the ratio between the H_2 in the liquid phase and the active metal amount. This parameter has already been proved to be relevant [9, 14, 41].. In our experiments, both reducing (H_2) and oxidizing (O_2) agents were present at the same time in the reaction environment and, of course, both can affect the Pd surface. However, the ratio between the concentration of dissolved reagents (H_2 and O_2) and available Pd varies. O_2 was always present in large excess, so that O_2/H_2 molar ratio[55] in the liquid phase was always higher than 15. In spite of this, no catalyst was ever fully oxidized at the end of the reaction and even some reduction was observed. This suggests that the key factor controlling the selectivity is rather the molar ratio between the H_2 dissolved in the liquid phase (H_2^L) and the quantity of Pd. We correlate the total amount of palladium with the H_2 solubilised in the liquid phase and not only the nanocluster surface because of the experimental evidence that the H_2O_2 selectivity may be impaired by the formation of palladium β-hydrides [56] . The β-hydrides can be formed also beneath the metal surface so that the composition of the interior of the nanoparticles can be relevant to the selectivity, too. Moreover, in this study the amount of the surface palladium is directly proportional to its total amount (Supplementary Information Figure 4). For these reasons the value of H_2^L/Pd is a proper parameter to compare the catalyst activity. In a batch reactor this ratio steadily decreases as the reaction proceeds, so that its initial value will be used hereafter. The initial H_2 concentration in the liquid phase was calculated as the H_2 concentration in equilibrium with the initial gas phase composition[55]. We have already reported that the initial H_2^L/Pd molar ratio plays an important role in the H_2O_2 direct synthesis[13, 41]. Here we have found that in both sets of catalytic runs, higher H_2^L/Pd values favour the production of H_2O_2 (Figure 8a). This is in agreement with our previous findings [9], where again a higher selectivity was achieved by decreasing the catalyst amount at constant H_2 concentration. Not surprisingly, the initial H_2^L/Pd ratio is correlated also with the Pd(II)/Pd(0) ratio in the spent catalysts (Figure 8b). In particular, when the initial value of H_2^L/Pd is relatively high the final Pd(II)/Pd(0) ratio is relatively low. The extent of metal oxidation during the reaction decreases also with the nanoparticle size (see above) and both factors certainly play a

Catalysis Science & Technology Accepted Manuscript

This journal is © The Royal Society of Chemistry 20xx

Please do not adjust margins

role. The final Pd(II)/Pd(0) ratio is not simply a matter of the initial H_2^L/Pd ratio; this is suggested by the value of Pd(II)/Pd(0) ratio in spent 1.0-Pd/K2621, which is *lower* than in the same fresh catalyst, although at the end of the reaction there is no more hydrogen. The higher resistance to oxidation of relatively large metal nanoparticles is also expected, because a relatively low dispersion implies the prevalence of low-index faces on the Pd surface, that are expected to be less reactive[33].

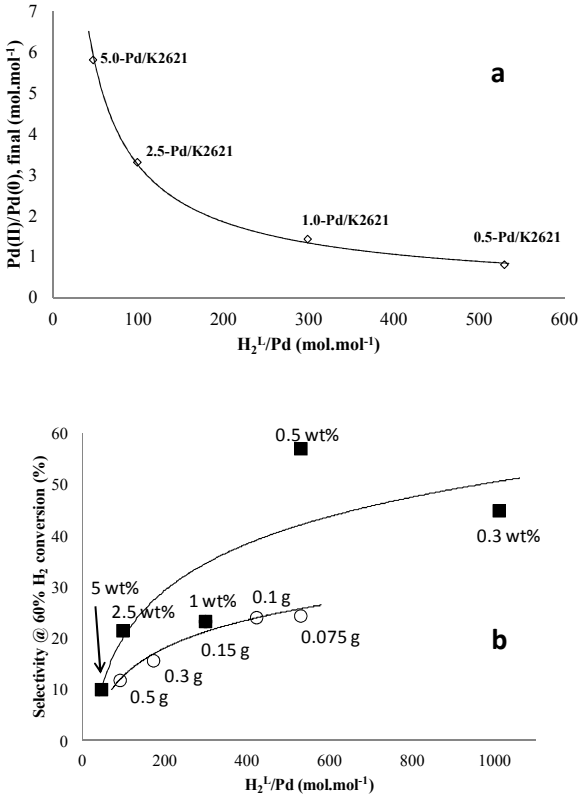

Figure 8. Selectivity at 60% H_2 conversion (a: ○ different amounts of 1.0 Pd/K2621; ■, different X Pd/K2621 catalyst; X= 0.3, 0.5, 1.0. 2.5, 5.0) and Pd(II)/Pd(0) molar ratio of spent catalysts (b) as a function of the H_2^L/Pd molar ratio.

Although we cannot clearly separate the effect of these parameters (i.e oxidation state, nanoparticle size, H_2^L/Pd initial value), we conclude that the combination of a relatively high H_2^L/Pd initial value (i.e. low catalyst amount) with relatively large metal nanoparticles is recommended to improve the selectivity towards H_2O_2. These conditions contribute to a low oxidation degree of the active metal, which appears beneficial to the selectivity. The positive effect of Pd reduction was also reported by Biasi *et al.*[41] , Burato *et al.*[23] , Melada *et al.*[24] and Liu *et al.*[25] . As already reported in the literature[57-61], there exists a competition in the sorption phenomena between oxygen and hydrogen on the catalyst surface. The sorption extent and rate depend on the metal cluster size and metal oxidation state[62-67]. For these reasons the H_2^L/Pd initial value is an important parameter that affects the sorption phenomena.
Summarizing, it was demonstrated that the different initial H_2^L/Pd molar ratio, along with the Pd nanoparticle size, can determine different oxidation state of the catalyst, eventually controlling the relative rates of H_2O and H_2O_2 production, i.e. the instantaneous selectivity of the catalyst.

Conclusions

The results reported in this work show that in the direct synthesis of hydrogen peroxide the H_2^L/Pd ratio is a key factors in controlling the rates of H_2O and H_2O_2 production over monometallic Pd catalysts supported on the commercial ion-exchange resin K2621 in the absence of promoters (halides and acids). This work successfully demonstrated that a low Pd(II)/Pd(0) molar ratio (i.e a more reduced catalyst) has a positive effect on the production of H_2O_2. A high H_2^L/Pd ratio, helping to reduce the catalyst, and a relatively low dispersion of the metal phase, which makes it more resistant to oxidation, are fundamental conditions to obtain an active catalyst for the direct synthesis. In fact, the 0.5-Pd/K2621, which is the least oxidized catalyst and has the largest nanoparticles, was the most selective when operating at H_2^L/Pd =530 (the second highest value in this investigation), with 57 % selectivity at 60 % conversion of H_2 (up to 80 % at lower conversion) and an H_2O_2 productivity of 12.4 mol·h^{-1} (corresponding to a specific peroxide productivity of 1313 molH_2O_2·molPd^{-1}·h^{-1}). These are interesting results using a monometallic Pd catalyst in the absence of promoters. Further investigations are required to explain why less oxidized Pd is more selective and how its oxidation can be even more effectively limited, in order to achieve high selectivity and H_2O_2 concentration also at high H_2 conversions. Most remarkably, structure sensitivity in H_2O_2 production and structure insensitivity in the H_2O production were noticed in the direct synthesis reaction network. This discovery will open new insights in the reaction mechanism of the direct synthesis.

Experimental Section

Materials

Lewatit K2621 (sulfonated polystyrene-divinylbenzene macroreticular ion-exchange resin; exchange capacity = 1.92 mmol·g-1) was provided by Lanxess. Pd(NO3)2 (Alfa Aesar) was used as received. Tetrahydrofuran (THF, Sigma-Aldrich) used freshly distilled. HPLC grade (99.99%) methanol for HPLC is from J.T. Baker. H2 and O2 as reagents and CO2 as an inert gas (AGA-Linde 5.0 purity) were used in the direct synthesis experiments.

Catalyst preparation

Pd supported on K2621 materials were prepared by ion exchange method. The reduction of the precursors to the metals takes place inside the polymer framework, which is able to control the dispersion, the size and, therefore, the catalytic properties of the metal nanoparticles. Lewatit K2621 is a macroreticular, sulfonated polystyrene-divinylbenzene (S-PSDVB) resin. It possesses permanent meso- and macropores both in the dry and in the swollen states. The permanent

Catalysis Science & Technology Accepted Manuscript

Please do not adjust margins

meso- and macropores of macroreticular resins make the diffusion of reagents and products less dependent on the swelling and generally faster. Thus, Lewatit K2621, with its macroporous structure and its ability to swell in polar solvents should be suited to overcome internal mass transfer limitations. Moreover, its acidic nature (exchange capacity is 1.92 mmol/g) appears to provide the same functionality of added acids, avoiding the use of a corrosive reaction environment[22, 23]. Overall, S-PSDVB resins have several features making them attractive supports for the direct synthesis catalysts[68].

The resin K2621 was washed with water (300 ml for 10 g of material) and rinsed with methanol (100 ml for 10 g material). 2.0 g of K2621 was suspended in 10 ml of distilled water and left standing for 2 hours. An aqueous solution of $Pd(NO_3)_2$ was added to the suspension. The amount of $Pd(NO_3)_2$ was varied to obtain 0.3, 0.5, 1, 2.5 and 5 wt.% nominal Pd loadings, respectively (Table 4). After adding the metal solution, the suspension reacted overnight under mechanical stirring (swirling plate). The material was filtered and washed with deionized water (5 x 10 ml). The mother liquors were analyzed for the unreacted metal by means of inductively coupled plasma mass spectrometry (ICP-MS). The residual amount of metal after the ion-exchange was always less than 0.1 mol % of the initial amount, confirming that the actual metal loadings were essentially equal to the nominal values. The as synthesized materials were suspended in THF and reduced under H_2 flux, at room temperature, for 5 hours. After recovery by vacuum filtration, the materials were washed on filter paper with THF (3 x 10 ml) and dried at 110°C overnight.

Catalyst	K2621/H^+ (g)	$Pd(NO_3)_2$ (g)	Measured Pd loading (wt.%)
0.3-Pd/K2621	10.6705	0.0875	0.30
0.5-Pd/K2621	1.1702	0.0174	0.52
1.0-Pd/K2621	5.2103	0.1375	1.03
2.5-Pd/K2621	1.0256	0.0668	2.56
5.0-Pd/K2621	1.0189	0.1314	5.07

Table 4. Analytical data on Pd catalysts with different metal loadings.

Characterization method

All XPS spectra were recorded with Kratos Axis Ultra electron spectrometer equipped with a delay line detector. A monochromated Al Kα source operated at 150 W, hybrid lens system with magnetic lens, proving an analysis area of 0.3 x 0.7 mm2, and charge neutralizer were used for the measurements. The binding energy (BE) scale was referenced to the C1s line of aliphatic carbon, set at 285.0 eV. Processing of the spectra was accomplished with the Kratos software. An Al Ka X-rays was used as excitation source with photon energy of 1486,6 eV. Depth of analysis for our samples is 10 nm and is not dependent on excitation source in conventional XPS.

Active metal content in the reaction medium was accessed by a PerkinElmer Sciex ICP Mass Spectrometer Elan 6100 DRC Plus. The timing parameters were: Sweeps/Reading: 11, Readings/Replicate: 1, Number of Replicates: 7, Dwell time: 50.0 ms, Scan mode: Peak Hopping. The calibration solutions were prepared from commercial single element solution for Pd, diluted into standard serial from 1 ppb to 100 ppb.

TEM analyses were carried out with an energy filtered transmission electron microscopy (EFTEM, LEO 912 OMEGA, LaB6 filament, 120 kV). Samples were prepared by suspending a few milligrams of the powder in high purity isopropyl alcohol (or ethanol). After ultrasonic bath (30 s) a small droplet (5 µl) of the suspension was transferred onto a holey-carbon film coated Cu grids, which was eventually introduced into the microscope.

Catalytic tests

The catalysts were tested in a slurry, within an autoclave operated batchwise, following a common catalyst testing practice[19, 39, 69-71]. In a batch reactor the gas and the liquid composition and possibly the catalyst state change over time. This is the same as the variations along the flow direction in continuous flow reactors[12]. Reactors where the gas is continuously bubbled through a well-mixed slurry provide approx. constant H_2 and O_2 concentration in the slurry, but still the products (which can be reagents for side reactions, such a H_2O_2) change concentration over time and the catalyst may vary its state. Thus, the batch reactor leads to a more complicated, but feasible kinetic analysis[14] while allowing for a rapid comparison of catalysts, even if differences in the reaction environment at the same elapsed time may occur. These are expected to be fairly small when comparing similar catalysts.

The catalysts were analyzed before and after the reaction, to correlate the reaction conditions to the possible variation of the catalyst properties. Hydrogen peroxide direct synthesis was performed in a 600 ml autoclave, described elsewhere[41]. Briefly, after the introduction of the catalyst, CO_2 and O_2 were fed to the reactor (partial pressures at 23 °C were 20.7 and 7.2 bar, respectively), followed by 420 ml of methanol. At this stage the internal pressure was 28 bars. The temperature decreased to 2 °C and stirring (1000 rpm) started and kept for 30 min, allowing the gas-liquid equilibrium to be reached (lowering the pressure down to 19.5 bar). Then H_2 (0.0183 moles) was introduced in the reactor as the limiting reagent from a reservoir of known volume and the reaction was started. The measured pressure drop in the H_2 reservoir allowed for a precise and reproducible determination of the amount of H_2 introduced in the reactor. Several liquid samples were withdrawn through a GC-valve during each experiment. H_2O_2 and H_2O concentrations were determined by iodometric and Karl-Fischer titrations, respectively. The H_2O_2 selectivity was calculated as follows: H_2O_2 selectivity = (moles H_2O_2

Catalysis Science & Technology Accepted Manuscript

 This journal is © The Royal Society of Chemistry 20xx

Please do not adjust margins

produced) / (moles H_2O + H_2O_2 produced) x 100. Experiments were performed varying the total amount of Pd in the reaction system in two different ways. A first set of experiments was carried out using different amounts (0.075-0.500 g) of a single catalyst (1.0-Pd/K2621) in the same liquid volume, and a second set was carried out using always the same fixed amount (0.150 g) of different catalysts (Pd content 0.3-5.0 wt.%). All tests last 3 h.

Acknowledgements

Lanxess is kindly acknowledged for providing the K2621 resin. NG gratefully acknowledges the Cariparo Foundation in Italy and the Technology Development center of Finland (TEKES) for financial support. NG and SS gratefully acknowledge the Johan Gadolin Scholarship. PB gratefully acknowledges the Otto A. Malm Foundation and the Kempe Foundations for financial support. This work is part of the activities at the Åbo Akademi Process Chemistry Centre (PCC). Also, the Bio4Energy program is acknowledged.

References

1 C. Samanta, *Applied Catalysis A: General,* 2008, **350**, 133-149.

2 J. K. Edwards, S. J. Freakley, R. J. Lewis, J. C. Pritchard and G. J. Hutchings, *Catalysis Today,* 2015, **248**, 3-9.

3 T. M. Rueda, J. G. Serna and M. J. C. Alonso, *The Journal of Supercritical Fluids,* 2012, **61**, 119-125.

4 P. Biasi, S. Zancanella, F. Pinna, P. Canu and T. O. Salmi, *Chem. Eng. Trans.,* 2011, **24**, 49-54.

5 P. Biasi, F. Menegazzo, F. Pinna, K. Eränen, T. O. Salmi and P. Canu, *Chem. Eng. J.,* 2011, **176-177**, 172-177.

6 T. Deguchi and M. Iwamoto, *Industrial and Engineering Chemistry Research,* 2011, **50**, 4351-4358.

7 T. Inoue, Y. Kikutani, S. Hamakawa, K. Mawatari, F. Mizukami and T. Kitamori, *Chem. Eng. J.,* 2010, **160**, 909-914.

8 S. Abate, M. Freni, R. Arrigo, M. E. Schuster, S. Perathoner and G. Centi, *ChemCatChem,* 2013, **5**, 1899-1905.

9 P. Biasi, J. Garcia-Serna, A. Bittante and T. Salmi, *Green Chem.,* 2013, **15**, 2502-2513.

10 J. K. Edwards, S. J. Freakley, A. F. Carley, C. J. Kiely and G. J. Hutchings, *Acc. Chem. Res.,* 2014, **47**, 845-854.

11 P. Biasi, F. Menegazzo, F. Pinna, K. Eränen, P. Canu and T. O. Salmi, *Ind. Eng. Chem. Res.,* 2010, **49**, 10627-10632.

12 S. J. Freakley, M. Piccinini, J. K. Edwards, E. N. Ntainjua, J. A. Moulijn and G. J. Hutchings, *ACS Catal.,* 2013, **3**, 487-501.

13 J. Garcia-Serna, T. Moreno, P. Biasi, M. J. Cocero, J. Mikkola and T. O. Salmi, *Green Chem.,* 2014, **16**, 2320.

14 N. Gemo, P. Biasi, P. Canu and T. O. Salmi, *Chemical Engineering Journal,* 2012, **207–208**, 539-551.

15 I. Huerta, J. García-Serna and M. J. Cocero, *The Journal of Supercritical Fluids,* 2013, **74**, 80-88.

16 Y. Voloshin and A. Lawal, *Applied Catalysis A: General,* 2009, **353**, 9-16.

17 Y. Voloshin, J. Manganaro and A. Lawal, *Industrial and Engineering Chemistry Research,* 2008, **47**, 8119-8125.

18 T. Deguchi and M. Iwamoto, *Journal of Catalysis,* 2011, **280**, 239-246.

19 J. K. Edwards, J. Pritchard, M. Piccinini, G. Shaw, Q. He, A. F. Carley, C. J. Kiely and G. J. Hutchings, *Journal of Catalysis,* 2012, **292**, 227-238.

20 V. R. Choudhary, S. D. Sansare and A. G. Gaikwad, *Catalysis Letters,* 2002, **84**, 81-87.

21 V. Choudhary, A. Gaikwad and S. Sansare, *Catalysis Letters,* 2002, **83**, 235-239.

22 G. Blanco-Brieva, E. Cano-Serrano, J. Campos-Martin and J. L. G. Fierro, *Chem. Commun.,* 2004, **0**, 1184-1185.

23 C. Burato, P. Centomo, M. Rizzoli, A. Biffis, S. Campestrini and B. Corain, *Advanced Synthesis & Catalysis,* 2006, **348**, 255-259.

24 S. Melada, R. Rioda, F. Menegazzo, F. Pinna and G. Strukul, *Journal of Catalysis,* 2006, **239**, 422-430.

25 Q. Liu, K. Gath, J. Bauer, R. Schaak and J. Lunsford, *The Active Phase in the Direct Synthesis of H_2O_2 from H_2 and O_2 over Pd/SiO_2 Catalyst in a H_2SO_4/Ethanol System*, Springer Netherlands, 2009.

26 R. Arrigo, M. E. Schuster, S. Abate, S. Wrabetz, K. Amakawa, D. Teschner, M. Freni, G. Centi, S. Perathoner, M. Hävecker and R. Schlögl, *ChemSusChem,* 2014, **7**, 179-194.

27 K. Jeřábek, L. Hanková and L. Holub, *Journal of Molecular Catalysis A: Chemical,* 2010, **333**, 109-113.

28 B. Corain, M. Zecca, P. Canton and P. Centomo, *Synthesis and catalytic activity of metal nanoclusters inside functional resins: an endeavour lasting 15 years*, 2010.

29 L. Ouyang, P. Tian, G. Da, X. Xu, C. Ao, T. Chen, R. Si, J. Xu and Y. Han, *Journal of Catalysis,* 2015, **321**, 70-80.

Catalysis Science & Technology Accepted Manuscript

Please do not adjust margins

30 B. D. Ratner and D. G. Castner, in *Surface Analysis - The Principal Techniques*, ed. nonymous , John Wiley & Sons, Ltd, 2009, p. 47-112.

31 C. R. Lederhos, J. M. Badano, N. Carrara, F. Coloma-Pascual, M. C. Almansa, D. Liprandi and M. Quiroga, *Metal and Precursor Effect during 1-Heptyne Selective Hydrogenation Using an Activated Carbon as Support*, 2013.

32 Moulder, John F., Chastain, Jill., King,Roger C., *Handbook of x-ray photoelectron spectroscopy : a reference book of standard spectra for identification and interpretation of XPS data*, Physical Electronics, Eden Prairie, Minn., 1995.

33 S. Penner, P. Bera, S. Pedersen, L. T. Ngo, J. J. W. Harris and C. T. Campbell, *J Phys Chem B,* 2006, **110**, 24577-24584.

34 J. M. Campos-Martin, G. Blanco-Brieva and J. L. G. Fierro, *Angewandte Chemie International Edition,* 2006, **45**, 6962-6984.

35 J. K. Edwards, A. Thomas, A. F. Carley, A. A. Herzing, C. J. Kiely and G. J. Hutchings, *Green Chem.,* 2008, **10**, 388-394.

36 G. Li, J. Edwards, A. F. Carley and G. J. Hutchings, *Catalysis Today,* 2007, **122**, 361-364.

37 G. Bernardotto, F. Menegazzo, F. Pinna, M. Signoretto, G. Cruciani and G. Strukul, *Applied Catalysis A: General,* 2009, **358**, 129-135.

38 G. Blanco-Brieva, F. E. de, J. Campos-Martin and J. L. G. Fierro, *Green Chem.,* 2010, **12**, 1163-1166.

39 S. Abate, P. Lanzafame, S. Perathoner and G. Centi, *Catalysis Today,* 2011, **169**, 167-174.

40 P. Biasi, P. Canu, F. Menegazzo, F. Pinna and T. O. Salmi, *Ind. Eng. Chem. Res.,* 2012, **51**, 8883-8890.

41 P. Biasi, N. Gemo, J. R. Hernández Carucci, K. Eränen, P. Canu and T. O. Salmi, *Industrial and Engineering Chemistry Research,* 2012, **51**, 8903-8912.

42 G. C. Bond, *Chem. Soc. Rev.,* 1991, **20**, 441-475.

43 M. Che and C. O. Bennett, *Advances in Catalysis,* 1989, **36**, 55-172.

44 R. A. Van Santen, *Acc. Chem. Res.,* 2009, **42**, 57-66.

45 H. S. Taylor, *Proceedings of the Royal Society of London A: Mathematical, Physical and Engineering Sciences,* 1925, **108**, 105-111.

46 M. Boudart, A. Aldag, J. E. Benson, N. A. Dougharty and C. Girvin Harkins, *Journal of Catalysis,* 1966, **6**, 92-99.

47 M. Boudart and F. Rumpf, *Reaction Kinetics and Catalysis Letters,* 1987, **35**, 95-105.

48 B. Lang, R. W. Joyner and G. A. Somorjai, *Surf. Sci.,* 1972, **30**, 454-474.

49 D. W. Blakely and G. A. Somorjai, *Journal of Catalysis,* 1976, **42**, 181-196.

50 G. A. Somorjai, *Acc. Chem. Res.,* 1976, **9**, 248-256.

51 J. T. Yates, *Journal of Vacuum Science & Technology A,* 1995, **13**, 1359-1367.

52 W. M. Lemke, R. B. Kaner and P. L. Diaconescu, *Inorg. Chem. Front.,* 2015, **2**, 35-41.

53 Ş Sarioğlan, *Platinum Metals Rev.,* 2013, **57**, 289.

54 F. Zhao, M. Shirai, Y. Ikushima and M. Arai, *Journal of Molecular Catalysis A: Chemical,* 2002, **180**, 211-219.

55 N. Gemo, P. Biasi, T. O. Salmi and P. Canu, *The Journal of Chemical Thermodynamics,* 2012, **54**, 1-9.

56 F. Menegazzo, M. Manzoli, M. Signoretto, F. Pinna and G. Strukul, *Catalysis Today,* 2015, **248**, 18-27.

57 D. Söderberg and I. Lundström, *Solid State Commun.,* 1983, **45**, 431-434.

58 S. J. Teichner, *Applied Catalysis,* 1990, **62**, 1-10.

59 J. F. Lynch and T. B. Flanagan, *J. Phys. Chem.,* 1973, **77**, 2628-2634.

60 A. Baldi, T. C. Narayan, A. L. Koh and J. A. Dionne, *Nat Mater,* 2014, **13**, 1143-1148.

61 P. Dibandjo, C. Zlotea, R. Gadiou, C. Matei Ghimbeu, F. Cuevas, M. Latroche, E. Leroy and C. Vix-Guterl, *Int J Hydrogen Energy,* 2013, **38**, 952-965.

62 M. Shao, T. Yu, J. H. Odell, M. Jin and Y. Xia, *Chem. Commun.,* 2011, **47**, 6566-6568.

63 S. Kim, D. Lee and K. Lee, *Journal of Molecular Catalysis A: Chemical,* 2014, **391**, 48-54.

64 S. Kim, D. Lee and K. Lee, *Journal of Molecular Catalysis A: Chemical,* 2014, **383–384**, 64-69.

65 M. Shao, *J. Power Sources,* 2011, **196**, 2433-2444.

66 S. Huang, C. Huang, B. Chang and C. Yeh, *J Phys Chem B,* 2006, **110**, 21783-21787.

Catalysis Science & Technology Accepted Manuscript

This journal is © The Royal Society of Chemistry 20xx

Please do not adjust margins

67 C. Nützenadel, A. Züttel, D. Chartouni, G. Schmid and L. Schlapbach, *The European Physical Journal D,* 2000, **8**, 245-250.

68 S. Sterchele, P. Biasi, P. Centomo, P. Canton, S. Campestrini, T. Salmi and M. Zecca, *Applied Catalysis A: General,* 2013, **468**, 160-174.

69 B. E. Solsona, J. K. Edwards, P. Landon, A. F. Carley, A. Herzing, C. J. Kiely and G. J. Hutchings, *Chem. Mater.,* 2006, **18**, 2689-2695.

70 F. Menegazzo, M. Signoretto, M. Manzoli, F. Boccuzzi, G. Cruciani, F. Pinna and G. Strukul, *Journal of Catalysis,* 2009, **268**, 122-130.

71 C. Burato, S. Campestrini, Y. Han, P. Canton, P. Centomo, P. Canu and B. Corain, *Applied Catalysis A: General,* 2009, **358**, 224-231.

Catalysis Science & Technology Accepted Manuscript

Please do not adjust margins